KSCE Journal of Civil Engineering (2016) 20(4):1267-1282

DOI 10.1007/s12205-015-0767-6

Geotechnical Engineering

pISSN 1226-7988, eISSN 1976-3808
www.springer.com/12205

Shear Zone Evolution of Granular Soils in Contact with Conventional and Textured CPT Friction Sleeves

G. L. Hebeler*, A. Martinez, and J. D. Frost*****

Received November 6, 2014/Revised 1st: April 20, 2015, 2nd May 13, 2015/Accepted May 22, 2015/Published Online

Abstract

Interfaces, and the shearing of soil against them, play a crucial role in geotechnical engineering. As such, understanding the fundamental mechanisms of interface behavior, such as the size, shape, and extent of soil shear zones against geomaterial surfaces can lead to better understanding and design of geotechnical systems and testing methods. The current study presents a series of laboratory studies aimed at spatially quantifying shear zones created through soil – geomaterial interface shearing including mobilized interface strengths with a focus on CPT friction sleeve behavior. Parametric investigations of particle shape and size effects were carried out over a range of counterface surface roughness values. The results show that conventional "smooth" CPT friction sleeves induce solely particle sliding in coarse grained soils, while non-clogging textured friction sleeves can create a combination of particle shearing and sliding that can allow for direct interface measurements in-situ. By varying the amount of texture on an interface, the extent of particle shearing can be controlled, allowing for improved understanding and treatment of interfaces in geotechnical testing and design.

Keywords: *interface shearing, shear zone evolution, CPT, friction sleeve, roughness, granular, particulate – continuum interface*

1. Introduction

Interface shearing is a primary consideration in a range of geotechnical issues. Common geotechnical problems such as pile design, slope stability, micro tunneling, earth retaining structures, landfill liners and many others are dependent on the strength of soil-geomaterial interfaces. Additionally, many laboratory and in-situ testing techniques are influenced by interface behavior or were designed to directly measure interface response, including: triaxial, resonant column, torsional shear, interface shear, standard penetration, borehole shear, and cone penetration testing. While interfaces have increasingly become an area of research and practice interest, a complete understanding of interface shearing mechanics has yet to be fully presented in the geotechnical literature, and common geotechnical design methodologies still primarily rely on empirical relationships to account for interface behavior. Additionally, the design of testing devices often ignores or has only been recently improved to appropriately deal with the effects of interface mechanics on the effectiveness of the test setup. Because interfaces, and the shearing of soil against them, play such an important role across all aspects of geotechnical engineering, it is imperative to understand the mechanisms of interface processes in order to enable improved geotechnical test and design methods.

The beginning of modern interface research as it pertains to geotechnical engineering was initiated by Potyondy (1961) and Brumund and Leonards (1973). These early studies demonstrated the importance of the soil's moisture content, particle angularity, particle size, mineralogy, and normal load on interface strength. The most commonly accepted parameters for characterizing surface profile roughness in the geotechnical community are maximum roughness, R_{max}, and average roughness, R_a. R_{max} is the absolute vertical distance between the highest peak and lowest valley along a surface profile and R_a is the average vertical relief over a specified sample length. A thorough discussion of measurement techniques and international standards for surface roughness characterization can be found in Ward (1999), with a detailed discussion focused on geotechnical applications in DeJong *et al.* (2002). Quantification of the role of surface roughness on particulate-continuum interfaces was pioneered by Uesugi and Kishida (1986a, 1986b), through their laboratory work on sand-steel interfaces. Using a normalized roughness parameter, R_n (defined as R_{max} normalized by the mean particle diameter D_{50}), the surface roughness-interface shear strength

*Senior Geotechnical Engineer and Associate, Golder Associates, Atlanta, Georgia 30341, USA (E-mail: gregory_hebeler@golder.com)
**Graduate Research Assistant, School of Civil and Environmental Engineering, Georgia Institute of Technology, Atlanta, Georgia 30332-0355, USA (Corresponding Author, E-mail: amartinez32@gatech.edu)
***Professor, School of Civil and Environmental Engineering, Georgia Institute of Technology, Atlanta, Georgia 30332-0355, USA (E-mail: david.frost@ce.gatech.edu)

relationship was found to be bilinear. The interface strength was shown to linearly increase, proportional to the increase in normalized roughness below a certain "critical" roughness value. Above the critical roughness, shear strength was observed to become constant and equal to the soil shear strength irrespective of roughness as the shearing transferred away from the interface into the adjacent soil mass. The measured interface shear strength was thus equal to the internal shear resistance of the contacting soil. The bilinear interface shear relationship has been shown to exist for a number of other geomaterial surfaces, including geomembranes, concrete, timber, and fiber reinforced polymers (Dove *et al*., 1997; Frost and Han, 1999; DeJong *et al*., 2000). Furthermore, the bilinear relationship has been shown to exist for other profile surface roughness parameters such as average roughness, R_a, and surface roughness, R_s (Lee, 1998) estimated using the tri-sector approach (Gokhale and Drury, 1990).

While partial motivation for the current study focuses on attempting to better understand the friction sleeve (f_s) measurements of conventional CPT devices, a significant impetus is linked to the extensive research focus on interface problems that has taken place both in the laboratory and in-situ during the preceding decades (Potyondy, 1961; Brumund and Leonards, 1973; Yoshimi and Kishida 1981a, 1981b; Uesugi and Kishida 1986a, 1986b; Uesugi *et al.*, 1988; Boulon 1989; Jardine and Lehane, 1993; Lehane and Jardine 1994; Jardine and Chow; 1996; Dove *et al*., 1997; Lee, 1998; Dove and Frost, 1999; Frost and Han, 1999; Frost *et al.*, 1999; Frost and Lee, 2001; White *et al*., 2001; Dietz and Lings, 2006; Wang *et al*., 2007; Ho *et al.*, 2011). Previous studies have attempted to document the spatial evolution of the shear zone during shearing; however, many of those studies have been limited by experimental influences or constraints. A summary of previous methods used to capture interface shear zone evolution include: the use of lead sphere inclusions. (Yoshimi and Kishida, 1981a); observation of the shear zone and individual particle tracking through an opaque side wall (Uesugi *et al.*, 1988 and White *et al*., 2001); monitoring of the individual contributions of sliding and shear deformation from simple shear loading (Uesugi and Kishida, 1986a); and the monitoring of clogged shear evolution (Hryciw and Irsyam, 1993). The current study uses an axisymmetric interface shear device developed by DeJong (2001) in combination with a heat-activated powdered phenolic resin to preserve the post-shear sand structure. The experiments provide quantitative insight into the development, evolution and spatial extent of the induced shear zones in addition to identifying the controlling shear mechanisms and the influence of mean particle size and characteristic angularity for both smooth and textured CPT friction sleeves.

One of the most common interface shear tests conducted in current geotechnical practice is the friction sleeve measurement (f_s) as part of the Cone Penetration Test (CPT). However, the results are used in practice with less frequency than other CPT measurements (Lunne *et al*., 1997). Some of the shortcomings of the f_s measurement are due to the design of the conventional CPT device including: the sleeve location within the highly stressed zone directly behind the CPT tip, the sleeve roughness (or lack thereof) and changes in roughness due to sleeve wear. The resulting large variability in measured values and associated poor correlation performance has limited usage of CPT f_s values in engineering practice.

In response to these shortcomings of the CPT friction sleeve measurement, a series of multi-sleeve friction penetrometer attachments has been developed by researchers at the Georgia Institute of Technology (DeJong, 2001; DeJong and Frost, 2002; Frost and DeJong, 2005; Hebeler, 2005; Hebeler and Frost, 2006). The first generation, or the Multi-Sleeve Friction Attachment (MFA), utilizes four independent friction mandrels with replaceable sleeves of varying surface roughness. The second generation, or the Multi-Piezo-Friction Attachment (MPFA), combines the benefits of four independent friction sleeve mandrels with five additional pore pressure sensors positioned before and after each sleeve location. The pore pressure measurements allow for an improved stratigraphic classification and to consider the friction sleeves within the effective stress framework. Both the MFA and MPFA were designed for use behind a conventional 15 cm^2 CPT device to allow for simultaneous determination of conventional CPT measurements (e.g., q_c, f_s, u_2) in conjunction with four individual interface shear measurements. Field testing at sites in the US and abroad has allowed for the performance of the devices to be fully evaluated and to establish their reliability and robustness. By configuring the MFA with sleeves of increasing roughness in series, the entire interface shearing – surface roughness relationship of a site can be characterized in a single sounding. An overlay of the friction sleeve measurements of such a sounding are shown in Fig. 1(a), with R_{max} = 0.25, 0.50, 1.00, and 2.00 mm for the four friction sleeves, respectively. Fig. 1(b) shows the bilinear relationship between interface strength and surface roughness derived from MFA field data. The latter

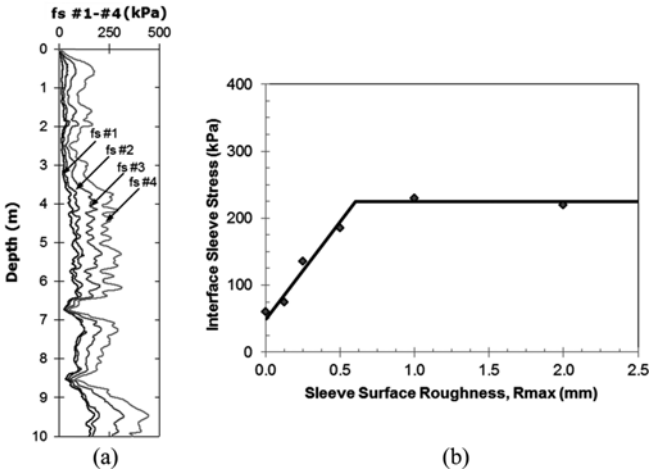

Fig. 1. (a) Overlay of Measured Sleeve Stress Obtained with MFA Configured with Sleeves Positioned in Order of Increasing Roughness (fs #1 is least rough and fs #4 is most rough) (b) In-situ Relationship between Surface Roughness and Interface Friction with the MFA (after DeJong, 2001)

has important implications for the integration of site characterization data in geotechnical design. Namely, if the designer knows the magnitude of the surface roughness of the material used for the geotechnical structure, they could refer to field results such as those presented in Fig. 1(b) and determine whether the inclusion-soil interface will mobilize the full soil internal strength or it will mobilize a fraction of it. This application represents a significant advantage for the design and analysis of deep foundations, earth retaining and micro tunneling, among others. Furthermore, a growing literature has presented studies that use data from the multi-sleeve penetrometers for applications such as the improved prediction of deep foundations skin friction capacity (Martinez, *et al.*, 2015) and the development of new soil classification charts (Frost and Martinez, 2013). The present study investigates the interactions between smooth and textured friction sleeves and and sands as well as the mobilized interface strengths considering the effect of the friction sleeve roughness magnitude, particle angularity and particle size. Conclusions are drawn from the results and implications regarding the resolution of field measurements and shear-induced soil response are described.

Within the content of this paper a conventional smooth CPT friction sleeve conforms to ASTM D 5578-12 and ISSMFE standards, which specify a friction sleeve roughness, R_a (average roughness), equal to 0.50 ± 0.25 μm. The sleeve texture pattern used in this study was designed to be "self-cleaning" to eliminate the possibility of soil particles clogging the texture and changing the surface roughness properties during testing. It was also found through extensive previous research that the optimum texturing pattern consists of features extending beyond a base substrate to allow for better soil engagement across the range of particles sizes and shapes encountered in situ (DeJong, 2001). Design considerations required that the textured sleeves induce internal shearing of the soil rather than only sliding along the surface, and that the texturing pattern should be easily machinable. The resultant texturing pattern consists of staggered diamond shaped elements with variations in their height used to modify the magnitude of surface roughness, with all other dimensions unchanged. The geometric configurations of the textured sleeves used in the current study are presented in Fig. 2. While texturing elements of different shapes were originally contemplated, diamond-shaped elements were selected because they were shown to successfully meet the above mentioned requirements, including their "self-cleaning" geometry, large soil engagement and ease of machinability (DeJong, 2001; DeJong and Frost, 2002). It is noted that using a different texturing pattern would possibly result in a different soil response being recorded, especially if such texture is prone to clogging, which would alter the sleeve-soil interactions throughout field and laboratory tests. On the other hand, the diamond shaped texturing is surrounded by sleeve areas with no textural features and thus surface characteristics equal to a conventional smooth CPT friction sleeve. The sections of smooth surface, referred to as "passthrough" zones, result in flow paths around/between each of the diamond asperities and prevent clogging of the textural features. For more information regarding the full progression of sleeve texture designs, including the use of different texturing elements such as ribs and diamonds of different widths, penetration angles and spacing configurations, refer to Cargill, 1999; DeJong *et al*., 2000; DeJong *et al.*, 2001; DeJong and Frost, 2002; Frost and DeJong, 2005.

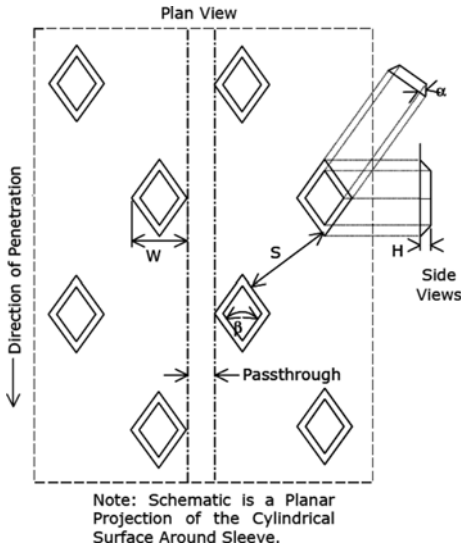

Fig. 2. Schematic of Diamond Texturing Pattern used to Creaty Varying Levels of Surface Roughness on Textured Friction Sleeves. H = Diamond Height, W = Diamond width, S = Diamond Spacing, α = angle and β = Penetration Angle (after DeJong, 2001)

2. Experimental Methods and Testing Materials

The experimental equipment used in the current test program consisted of an axisymmetric interface shear apparatus developed

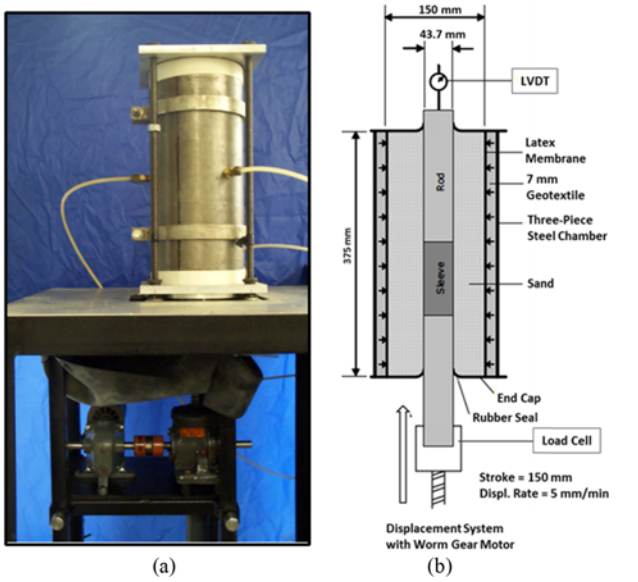

Fig. 3. Axisymmetric Shear Apparatus: (a) Photograph, (b) Schematic (after DeJong, 2001)

by DeJong (2001). This apparatus, shown in Fig. 3(a) and 3(b), allows for standard 43.7 mm diameter friction sleeves of any length to be mounted in the center of smooth sections of rod of the same diameter with standard average surface roughness equal to that of a conventional smooth CPT friction sleeves, R_a = 0.50 mm. The assembled test module is positioned at the center axis of a tri-part steel testing chamber and the sample is prepared around it, resulting into "perfect insertion" conditions that eliminate the disturbance caused by the tip insertion and associated cavity expansion observed in field or calibration chamber penetration tests. The inside of the chamber is lined with one layer of needle punched nonwoven geotextile and then a latex membrane which allows for constant lateral stress conditions during axisymmetric testing consistent with calibration chamber BC4 boundary conditions (Ghionna and Jamiolkowski, 1991). The upper and lower boundaries of the chamber consist of metal end platens with rubber seals at the center through which the test rod penetrates. A displacement system controlled by a worm gear motor is used at an average displacement rate of 5 mm/min (conforming to ASTM D 5321-14 standards for interface shear testing), and all samples are sheared for a total displacement of 63.5 mm. A constant lateral confining pressure of 50 kPa is applied to all specimens through three external ports, located at the center of each tri-mold section. Shear resistance loads were recorded by a load cell located between the bottom of the rod and the motor and the shear displacement was recorded by an LVDT located at the top end of the rod.

The soils used in the test program consisted of a local Atlanta blasting sand (sub-angular shape, G_s = 2.65, D_{50} = 0.72 mm, C_u = 1.25, roundness = 0.32) referred to as "sub-angular 20-30" sand throughout this paper, Ottawa 20-30 sand (sub-rounded shape, G_s = 2.65, D_{50} = 0.72 mm, C_u = 1.25, roundness = 0.73) referred to as "sub-rounded 20-30" sand, and 50-70 graded Ottawa sand (sub-angular shape, G_s = 2.65, D_{50} = 0.26 mm, C_u = 1.20, roundness = 0.50), referred as "sub-angular 50-70" sand. Figs. 4(a) through 4(c) show microscope images of the tested sands. The sub-angular 20-30 sand can be considered the control material in the current experiments, with the sub-angular 50-70 and sub-rounded 20-30 sands used to study the effects of particle size and angularity, respectively. Counterfaces tested in the current study consisted of a conventional smooth friction sleeve (R_a = 0.50 mm, R_{max} = 0.0064 mm) and four textured friction sleeves varying in surface roughness from R_a = 40 to 230 mm (R_{max} = 0.25 to 2.00 mm). The detailed specifications of the counterfaces used in the current study are listed in Table 1. It should be noted that the effect of other testing parameters such as sand relative density, magnitude of confining stress and magnitude of sleeve displacement were not investigated as part of this specific study but will be addressed in future research programs.

All of the sands were mixed with powdered phenolic resin at a concentration of 1% by weight. Samples were prepared dry, in thin lifts of 1 cm height using constant fall height air pluviation and light tamping, resulting in uniform specimens of medium relative density, between 60 and 70%. Natural and dyed layers of sand were alternated in the portion of the sample subjected to shearing against the sleeves in order to facilitate the visual study of soil particle deformations. The phenolic resin that was used to preserve the post-shear structure of the sand had no effect on the mechanical behavior of the granular materials during shearing, as shown by three control tests with and without phenolic resin that resulted in Coefficients of Variation (COV) lower than 5% for peak and residual recorded loads. It should be noted that this COV value also reflects other factors, such as local variations in density as shown by comparisons of two tests without resin that yielded COV values of about 3%. Further studies by means of direct shear tests (sample diameter = 2.5") yielded differences in

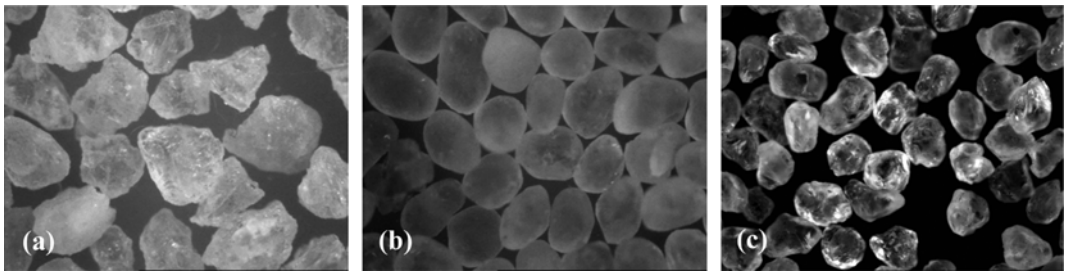

Fig. 4. Photographs of Test Sands: (a) Sub-angular 20-30, (b) Sub-rounded 20-30, (c) Sub-angular 50-70

Table 1. Summary of Smooth and Textured Sleeve Dimensions and Surface Roughness Values

Sleeve ID #	Height (H) (mm)	Pen. Angle (β) (deg)	Diagonal Spacing (S) (mm)	Percent Passthrough (%)	Width (W) (mm)	Angle (α) (deg)	R_{max} (mm)	R_a (mm)
SM	N/A	N/A	N/A	100	N/A	N/A	0.0064	0.0005
30H.25S3	0.25	60	6.3	15.7	5.3	45	0.25	0.066
30H.5S3	0.50	60	6.3	15.7	5.3	45	0.50	0.117
30H1S3	1.00	60	6.3	15.7	5.3	45	1.00	0.185
30H2S3	2.00	60	6.3	15.7	5.3	45	2.00	0.226

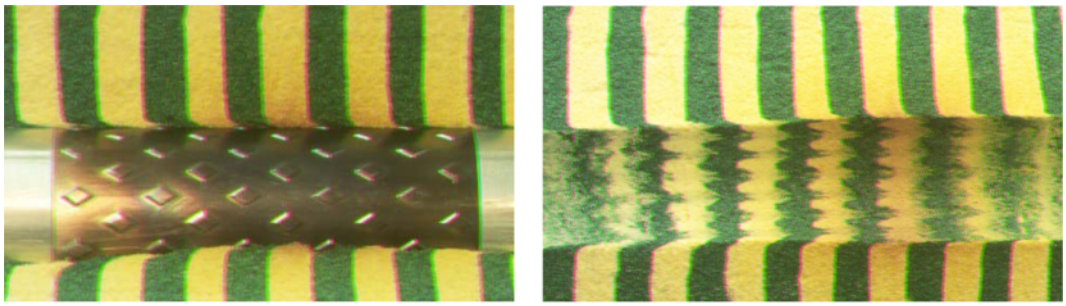

(a) (b)

Fig. 5. Picture of Post-Shear Preserved Sample (Sub-Angular 50-70 Sand) Sheared Against a Textured Sleeve (R_{max} = 0.5 mm), (a) Test Rod Still in Place, (b) Test Rod Removed

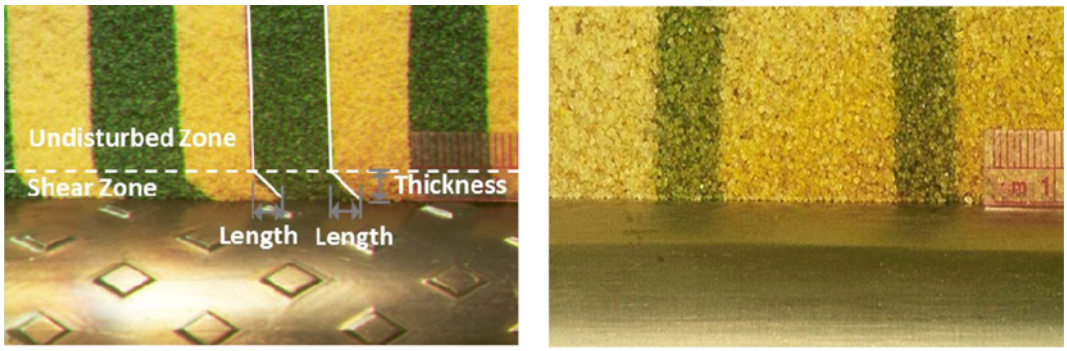

(a) (b)

Fig. 6. Pictures Showing the Preserved Post-shear Sand Structure of Axisymmetric Tests Against: (a) Textured Sleeve with Shear Zone, (b) Smooth Sleeve with no Shear Zone

peak and residual friction angles of less than 1° for tests with and without resin. After shearing, the entire specimen was heated above the melting point of the resin (150°-175°C) and then allowed to cool down, creating a light cementation at the particle contacts through the re-solidification of the melted resin. After cooling, each specimen was dissected in longitudinal slices along the displacement direction, such that a vertical face of the soil sample perpendicular to the rod axis was exposed for analysis. Examples of a sample dissection, with and without the rod in place are shown in Figs. 5(a) and 5(b), respectively, where the imprints of the texture elements can be observed in the latter image.

For samples with textured sleeves, investigation planes were centered either along the top of a column of diamond texture elements or within the passthrough space between the texture features. Furthermore, the initiation and progress of shear zone development was studied through the investigation of sand layers that experienced a combination of shearing against smooth and textured surfaces. Two deformation measurements were made for each dyed layer. The measurements are illustrated in Fig. 6(a) and consist of the distance radially away from the base sleeve surface (shear zone thickness), and the length along the contact surface where particle displacement was observed (shear zone length). Displacements were independently measured at both the leading and trailing edges of each colored layer and averaged to determine the average deformation of each layer. Photographs were taken with high resolution lenses to achieve high-quality images of the shear zones. Particle displacements were inventoried through measurement of the scaled digital images in AutoCAD®, allowing for a high precision record of all measurements.

3. Results

3.1 Results of Conventional Smooth Sleeve Shearing

Analysis of interface shearing with conventional smooth CPT friction sleeves was conducted using two techniques. For the tests with sub-rounded 20-30 sand, a complete interface shear test was performed with a smooth friction sleeve mounted between the top and bottom smooth rod sections. For the other granular materials (sub-angular 20-30 and 50-70) the reported smooth surface (R_a = 0.50 mm) deformations were taken from dyed layers continuously sheared against the top or bottom rod during the textured sleeve tests. These results are shown in Table 2. It can be observed that tests with sub-angular and sub-rounded 20-30 sands resulted in negligible shear zone deformation as shown in Fig. 6(b) for a test with sub-rounded 20-30 sand. However, tests with sub-angular 50-70 sand against a smooth sleeve resulted in a shear zone thickness of 4.2 D_{50} and a shear zone length of 2% of the total sleeve displacement.

3.2 Results of Textured Sleeve Shearing

For each test using a textured sleeve, conditions were such that different layers within the sample experienced different levels of

Table 2. Shear Zone Deformation Measurements for Smooth and Textured Friction Sleeves

Sand Type	R_{max} (mm)	R_a (mm)	R_n	Zone Thickness (mm)	Zone Thickness (D_{50} equiv.)	Zone Length (mm)	Zone Length (%)
Sub-Angular 20-30	0.006	5.E-04	0.01	0.0	0.0	0.0	0.0
	0.25	0.07	0.35	2.2	3.0	1.9	3.0
	0.50	0.12	0.69	3.7	5.0	4.6	7.2
	1.00	0.19	1.39	3.8	5.3	7.3	11.4
	2.00	0.23	2.78	4.5	6.2	14.6	23.0
Sub-Rounded 20-30	0.006	5.E-04	0.01	0.0	0.0	0.0	0.0
	0.25	0.07	0.35	2.6	3.6	2.5	3.9
	0.50	0.12	0.69	3.8	5.3	7.9	12.4
	1.00	0.19	1.39	4.5	6.2	8.3	13.1
	2.00	0.23	2.78	5.0	6.9	9.1	14.3
Sub-Angular 50-70	0.006	5.E-04	0.03	1.1	4.2	1.4	2.2
	0.25	0.07	0.96	2.5	9.6	3.6	5.6
	0.50	0.12	1.92	3.1	11.8	6.0	9.5
	1.00	0.19	3.85	3.8	14.8	12.8	20.1
	2.00	0.23	7.69	3.9	15.0	17.1	26.9

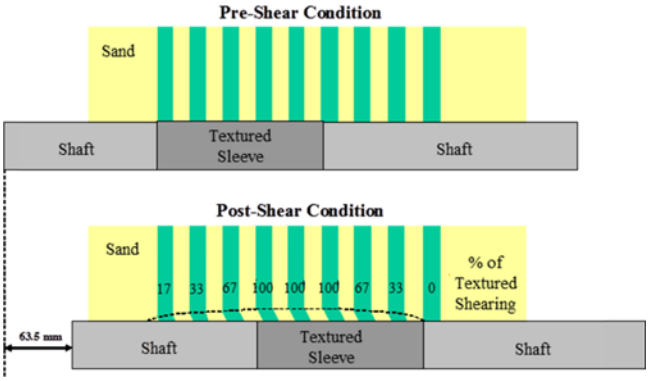

Fig. 7. Schematic Showing the Configuration of Colored Sand Layers Within Each Axisymmetric Test Sample

textured and smooth shearing. Layers were positioned such that three layers were kept in continuous contact with the textured sleeve. The remaining colored layers were positioned throughout the sample to experience either continuous smooth shearing or a combination of textured and smooth shearing over the entire displacement range. The position of the layers and the amount of textured shearing in terms of percentage of total sleeve displacement is shown in Fig. 7. The induced shear deformations for all tested surfaces and soils took the form of a simple shear failure condition in that all layers experienced relatively homogeneous shearing across the measured planar layer widths. Shear zone deformation results are presented as average layer deformations unless otherwise noted as in the discussion of shear zone uniformity. The results showed to be highly reproducible based on three control tests which yielded COV values of 4.9% for shear zone thickness and of 6.4% for shear zone length results. It should be noted that these COV values also reflect effects of other factors such as local variations in density.

The presented results (Table 2) allow the induced shear zone behavior to be observed as a function of variations in three distinct properties: the surface roughness (R_a and/or R_{max}) of the counterface materials, the mean particle diameter (D_{50}), and the average particle angularity. Variations in shear zone thickness for the various textured surfaces are presented in units of mm and equivalent multiples of mean particle size (D_{50}) allowing for direct and normalized comparisons. Similarly, variations in the induced shear zone length are presented both in terms of the measured deformation (mm) and as a percentage (%) of the total sleeve relative displacement (63.5 mm).

3.3 Mobilized Interface Shear Strength

The mobilized loads during the interface shear tests performed against friction sleeves of varying roughnesses are presented in Figs. 8(a) through 8(c) for sub-angular 20-30, sub-rounded 20-30 and sub-angular 50-70 sands, respectively. All the curves show peak load values at displacements smaller than 5 mm of sleeve displacement, followed by strain softening responses. The mobilized loads increase as surface roughness of the friction sleeves increases for the three sands.

As previously described by other researchers, the interface surface roughness and sand internal friction have a significant and direct impact on the mobilized interface shear strength and interface behavior (Potyondy, 1961; Uesugi and Kishida, 1986a and 1986b; Hryciw and Irsyam, 1993; Frost *et al*., 2002; Dietz and Lings, 2006). Figs. 9(a) and 9(b) present the mobilized peak and residual interface friction angles for tests on the three sands. The results show that both the mobilized peak and residual interface friction angles increase with increasing surface roughness for the three sands. The rate of increase decreases with increasing surface roughness, reaching more stable values at R_{max} values larger than 1.00 mm. The influence of the soil internal strength can also be observed since larger interface friction angles are mobilized by tests with the sub-angular 20-30 sand, followed by tests with sub-angular 50-70 and sub-rounded 20-30 sands. These results agree with the current understanding of

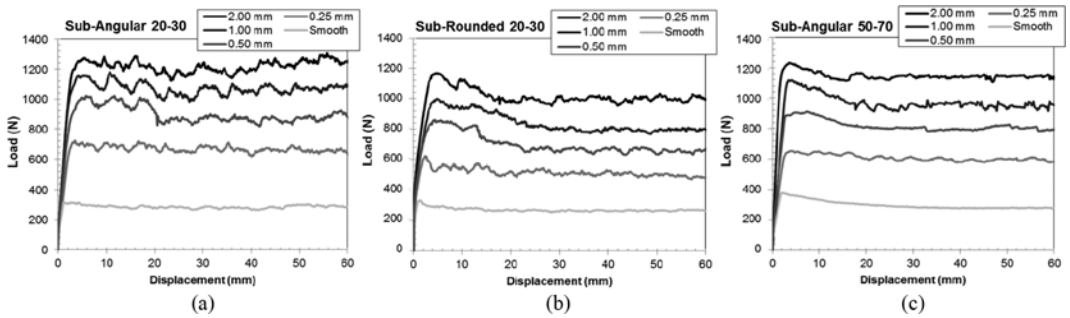

Fig. 8. Load-Displacement Curves for Tests Against Friction Sleeves of Varying Surface Roughness, R_{max}, on (a) Sub-Angular 20-30, (b) Sub-Rounded 20-30 and (c) Sub-Angular 50-70.

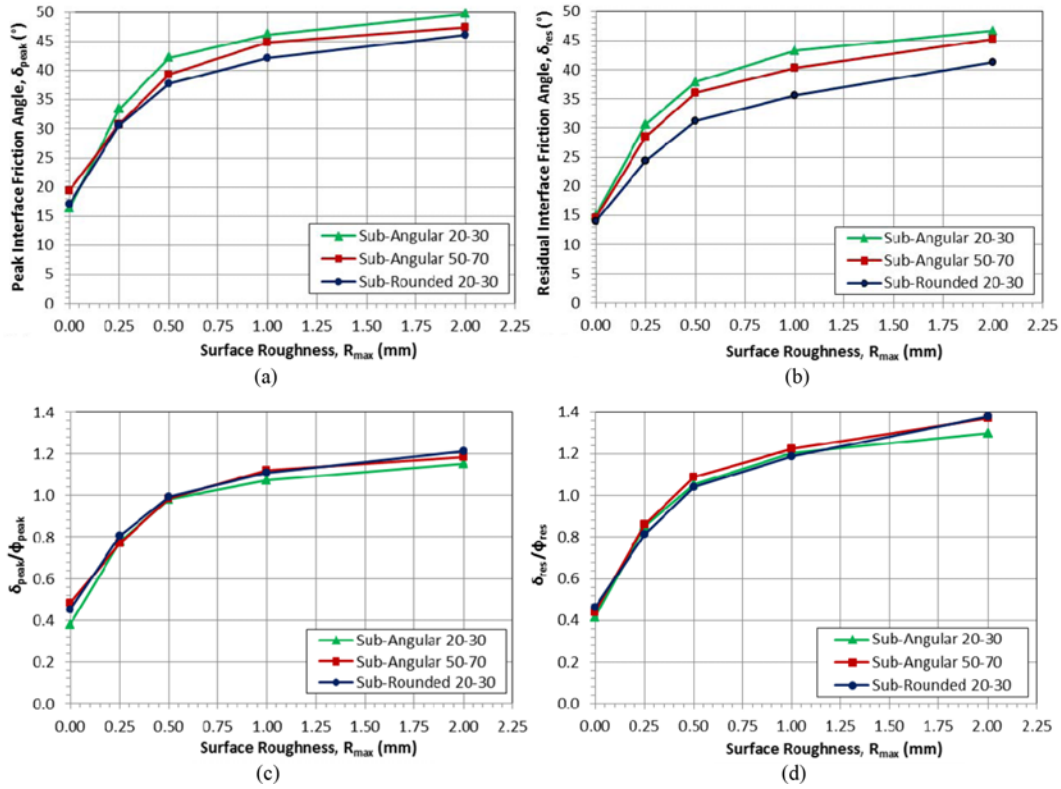

Fig. 9. Effect of Surface Roughness on Mobilized: (a) Peak, (b) Residual Interface Friction Angles and (c) Normalized Peak, (d) Normalized Residual Interface Friction Angles

interface behavior where sands of larger internal shear strengths mobilize larger interface shear strengths for any given surface roughness. It should be noted that the tests performed with conventional smooth CPT sleeves did not reflect the internal shear strength of the sands, as shown in Figs. 9(a) and 9(b). This observation reflects some of the shortcomings typically associated with the conventional f_s CPT reading (e.g. large variability in results as compared to the magnitude of measured loads). Additionally, these results highlight the advantages of using textured friction sleeves for site characterization purposes such as the direct measurement of soil internal strength.

Figures 9(c) and 9(d) show mobilized peak and residual interface friction angles normalized by corresponding peak and residual soil internal friction angles obtained from direct shear tests. As expected, the normalized interface friction angles increase with increasing surface roughness. It can be observed that at surface roughness values of 0.40 mm the normalized interface friction angles reach values larger than 1.0, meaning that the interface friction angles are greater than the internal soil friction angles. The reason for this is that the diamond elements of the textured sleeves mobilize passive resistances in addition to interface friction resistance, a situation that also takes place in soils reinforced with grid or ribbed reinforcements (Mitchell and Villet, 1987). Martinez, *et al*. (2015) presented a study on the interface friction and passive resistance load transfer mechanisms between sands and textured sleeves with diamond elements, including a methodology to isolate the interface friction and passive resistance components. The authors demonstrated that

after subtracting the contributions from passive resistances the interface friction angle values indeed converged to the value of the soil friction angle, yielding normalized interface friction angle values of 1.0.

3.4 Thickness and Length of Granular-Continuum Shear Zones

The measured shear zone thickness and shear zone length for the interface shear tests between all sands tested against smooth and textured sleeves are presented in Table 2. Figs. 10(a) and 10(b) show the shear zone thickness in terms of mm and D_{50} equivalents as a function of R_{max}, while Figures 10c and 10d present the same shear zone thickness results as a function of normalized roughness, R_n. These results show that increases in sleeve surface roughness results in concomitant increases in shear zone thickness, in a similar fashion as the interface friction angle results presented in Figs. 9(a) and 9(b). Also, the rate of increase in shear zone thickness decreases with increasing roughness, reaching a stable value at larger roughness values. The upper limits of shear zone thickness were determined to be between 4 and 5 mm for all sands tested, with normalized thicknesses on the order of 6 to 7 D_{50} equivalents and 12 to 14 D_{50} equivalents for the medium (D_{50} = 0.72 mm) and fine (D_{50} = 0.31 mm) sands, respectively.

The results presented in Figs. 10(e) and 10(f), in terms of R_{max} and R_n, respectively, indicate that increases in roughness also

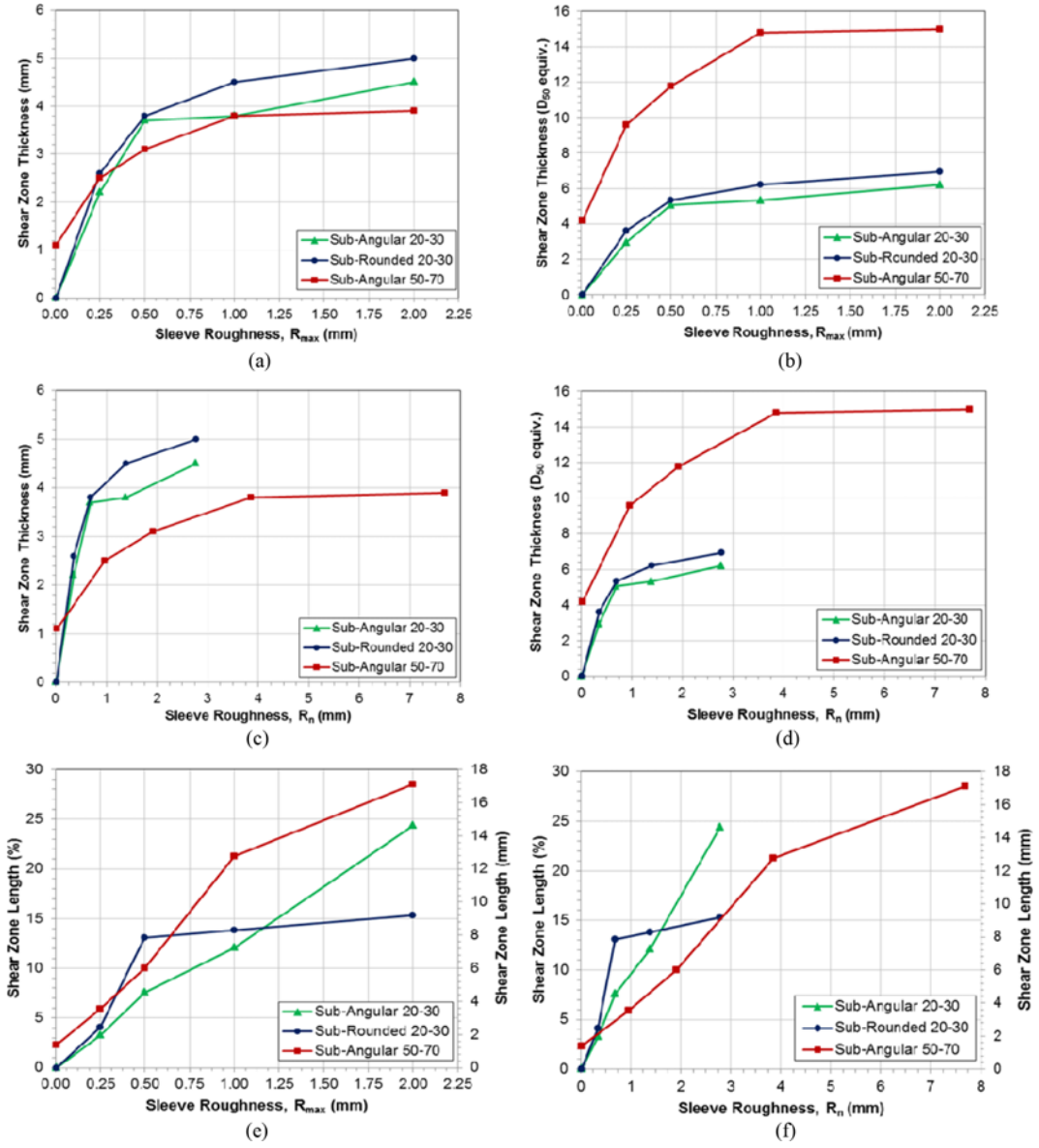

Fig. 10. Variation in Shear Zone Characteristics as a Function of Surface Roughness: (a) Shear Zone Thickness (mm) vs. Sleeve Roughness (R_{max}), (b) Shear Zone Thickness (D_{50} equivalents) vs. Sleeve Roughness (R_{max}), (c) Shear Zone Thickness (mm) vs. Sleeve Roughness (R_n), (d) Shear Zone Thickness (D_{50} equivalents) vs. Sleeve Roughness (R_n), (e) Shear Zone Length vs. Sleeve Roughness (R_{max}), (f) Shear Zone Length vs. Sleeve Roughness (R_n)

result in larger shear zone lengths. However, it can be observed that the tests with the sub-rounded sand reach a stable shear zone length value at large roughnesses, whereas the shear zone length for tests with sub-angular sands continued increasing with roughness over the range of relative displacements tested in this study. These results show that the use of the R_{max} parameter, along with the actual measured length, yield a better unification of the results, as shown in Figs. 10(a) and 10(e). Furthermore, previous studies by DeJong *et al*. (2002) have shown that the peak features of surfaces have a larger contribution towards the interface shear behavior than valley features. As such, the R_{max} parameter emphasizes the peak features of the textured friction sleeves, while R_a gives equal importance to both peaks and valleys since it is calculated as an average of all the features. Therefore, R_{max} is adopted as the roughness parameter for the presentation and discussion of results throughout the rest of this paper.

3.5 Uniformity of the Induced Shear Zones

The spatial uniformity of the induced shear zones was investigated by comparing the particle deformations along the tops of the diamonds with those along the passthrough space between vertical columns of diamond texture. As before, the results presented represent an average of all similar measurements taken for each specimen (Table 3). Figs. 11(a), 11(c) and 11(e) compare the top of diamonds and between diamond measurements of shear zone thickness for each of the granular materials, while Figs. 11(b), 11(d) and 11(f) show the associated shear zone length measurements. As previously noted, the current texturing scheme uses offset asperities of varying radial height to create friction sleeves of varying surface texture. While a non-continuous, non-uniform texturing scheme allows the surface texture to be non-clogging, there is the possibility of creating a non-uniform shear zone at different positions around the circumference of the textured sleeve.

As can seen from the figures and tabulated results, the induced shear zone thickness remains relatively constant circumferentially throughout the entire shear zone. The results for the two test sands with larger particles (Figs. 11(a) and 11(c)) showed only slight variations in measured shear zone thickness, with all variations less than one particle diameter. The sub-angular 50-70 sand (Fig. 11(e)), consisting of smaller particles, showed slightly higher variation in the shear zone thickness, especially at R_{max} = 1 mm. However, the shear zones at all other R_{max} values showed only minor variations in shear zone thickness throughout the shear zone. It is thus reasonable to conclude that the induced shear zones were of uniform thickness for the current testing parameters.

The induced shear zone lengths for the larger sand (sub-angular and sub-rounded 20-30) were homogeneous, with these being reduced on the order of 6% (or no more than 1 mean particle diameter) within the passthrough spaces compared to the deformation directly over the diamond asperities. As expected, the smaller sand (sub-angular 50-70) showed a much larger difference in shear zone length, with a reduction on the order of 24% along the passthrough space compared to that centered over the diamond texture (Fig. 11(f)). As the representative contacting particle diameter decreases, the passthrough space becomes larger with respect to the particle size. As a result, interaction between the particles within the passthrough space and along the line of texture decreases and the shear zone displacement subsequently becomes less uniform. This phenomenon will increase for soils of smaller diameter (e.g., silts and clays) than those tested herein.

3.6 Initiation and Progression of the Induced Shear Zones

In addition to the continuous shearing results, layers partially

Table 3. Shear Zone Deformation Measurements Detailing the Uniformity of the Induced Shear Zones

			Top of Diamonds				Between Diamonds				Average Values	
Sand Type	R_{max} (mm)	R_n	Zone Thickness (mm)	Zone Thickness (D_{50} equiv.)	Zone Length (mm)	Zone Length (%)	Zone Thickness (mm)	Zone Thickness (D_{50} equiv.)	Zone Length (mm)	Zone Length (%)	Zone Thickness (mm)	Zone Length (mm)
Sub-Angular 20-30	0.0064	0.01	0.0	0.0	0.0	0.0	0.0	0.0	0.0	0.0	0.0	0.0
	0.25	0.35	2.3	3.2	2.0	3.1	2.0	2.7	1.9	3.0	2.2	2.0
	0.50	0.69	3.7	5.1	4.8	7.5	3.6	5.0	4.3	6.7	3.7	4.6
	1.00	1.39	3.9	5.4	7.5	11.8	3.8	5.3	7	11.1	3.8	7.3
	2.00	2.78	4.6	6.4	14.6	23	4.3	6.0	14.6	23	4.5	14.6
Sub-Rounded 20-30	0.0064	0.01	0.0	0.0	0.0	0.0	0.0	0.0	0.0	0.0	0.0	0.0
	0.25	0.35	2.7	3.8	2.6	4.2	2.5	3.4	2.3	3.7	2.6	2.5
	0.50	0.69	3.9	5.4	8	12.6	3.8	5.3	7.7	12.2	3.8	7.9
	1.00	1.39	4.7	6.5	8.5	13.4	4.3	5.9	8.1	12.8	4.5	8.3
	2.00	2.78	5.0	7.0	9.6	15.1	4.9	6.9	8.8	13.9	5.0	9.2
Sub-Angular 50-70	0.0064	0.02	1.1	4.2	1.4	2.2	1.1	4.2	1.4	2.2	1.1	1.4
	0.25	0.96	2.6	9.8	4.1	6.5	2.5	9.4	3.0	4.8	2.5	3.6
	0.50	1.92	3.2	12.1	6.9	10.9	3.0	11.4	5.1	8.1	3.1	6.0
	1.00	3.85	4.1	15.8	14	22.1	3.6	13.8	11.5	18.2	3.8	12.8
	2.00	7.69	4.0	15.2	19.5	30.7	3.8	14.8	14.7	23.1	3.9	17.1

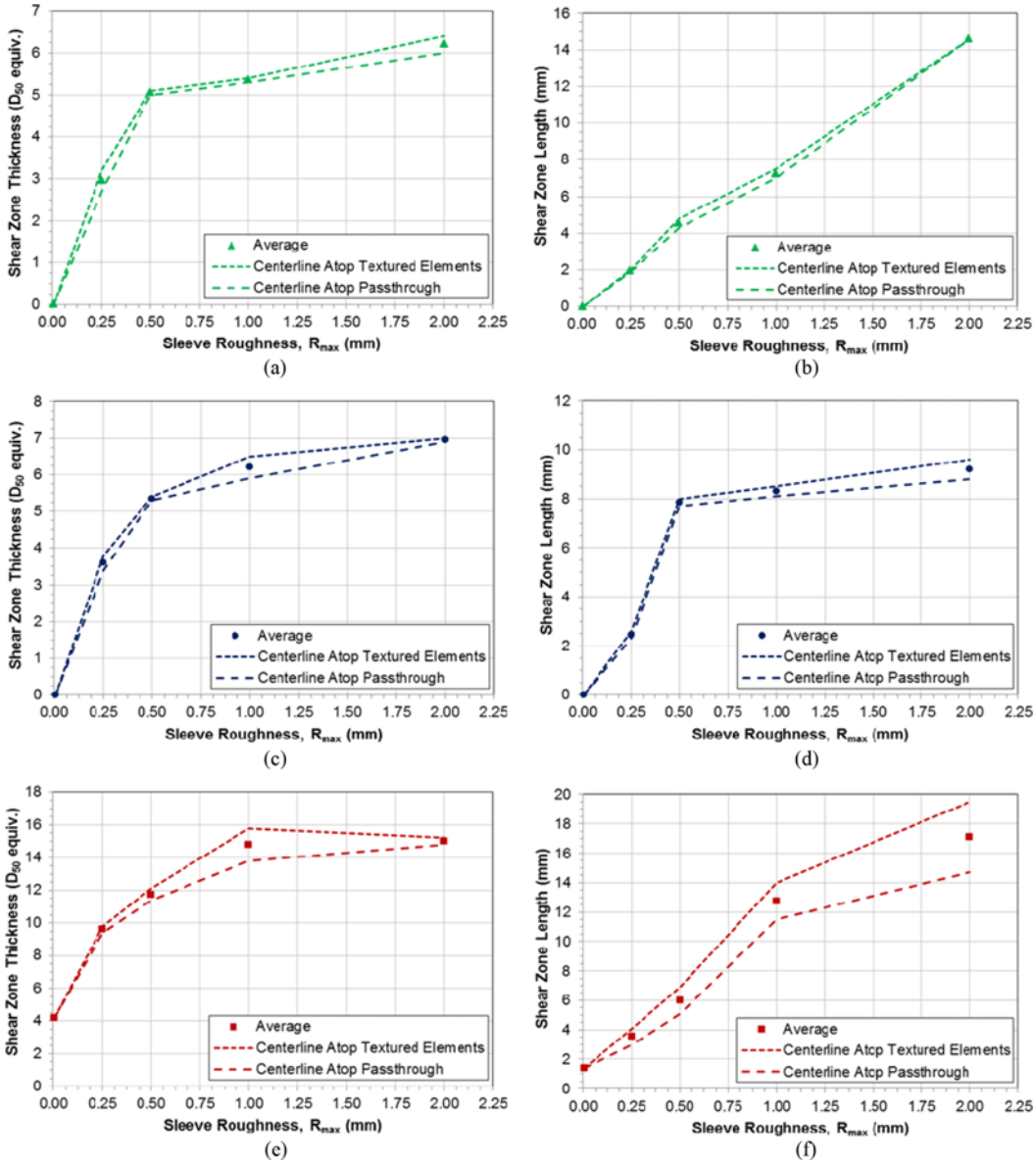

Fig. 11. Uniformity of Induced Shear Zone Thickness and Length as a Function of R_{max} for: (a) & (b) Sub-angular 20-30, (c) & (d) Sub-rounded 20-30 and (e) & (f) Sub-angular 50-70 Sands

sheared against the textured and smooth surfaces were used to investigate the initiation and progression of the induced shear zones. Not all specimens were prepared with the full nine layer configuration shown in Fig. 7 that allows for all possible shearing conditions to be investigated. Consequentially, shear zone progression is presented through comparisons of the shear zones induced from continuous textured shearing with shear zones induced from 67% and 33% textured shearing. These results are presented in Table 4 and Figs. 12(a) through 12(f).

The results show that full shear zone thickness is achieved after shearing against two paired rows of diamond texture (67% of the test displacement) (Figs. 12(a), 12(c) and 12(e)). Furthermore, Figs. 10(a) through 10(d) show the convergence to a constant shear zone thickness above a unique "critical" roughness level for each sand tested. This result leads to the potential future application of shortened friction sleeves for in-situ characterization with clear benefits for issues such as thin seam detection, as previously addressed by Saussus *et al.*, 2004. For the current sleeve texturing pattern, the minimum length required to induce fully formed shear zones appears to be equal to two rows of offset texture elements, on the order of 40 mm, as compared to lengths of 134 to 164 mm for sleeves complying with ASTM standards. It is noted that these historical lengths were dictated by the space needs of electronics in early penetrometer systems.

The sub-angular 20-30 and 50-70 sands exhibited further lengthening of the shear zones as the percentage of textured shear is increased (33% to 67% to 100%). Furthermore, the rate of increase of shear zone length is larger for rougher surfaces, as

Table 4. Shear Zone Formation and Progression Results

			33% Textured		67% Textured		100% Textured	
Sand Type	R_{max} (mm)	R_n	Zone Thickness (mm)	Zone Length (mm)	Zone Thickness (mm)	Zone Length (mm)	Zone Thickness (mm)	Zone Length (mm)
Sub-Angular 20-30	0.0064	0.01	N/A	N/A	N/A	N/A	0.0	0.0
	0.25	0.35	1.4	1.0	1.9	1.3	2.2	1.9
	0.50	0.69	N/A	N/A	3.4	3.3	3.7	4.7
	1.00	1.39	N/A	N/A	3.6	4.8	3.8	7.2
	2.00	2.78	N/A	N/A	4.2	7.2	4.5	14.5
Sub-Rounded 20-30	0.0064	0.01	N/A	N/A	N/A	N/A	0.0	0.0
	0.25	0.35	N/A	N/A	2.8	2.4	2.8	2.5
	0.50	0.69	2.7	2.5	3.9	5.6	3.8	8.0
	1.00	1.39	N/A	N/A	4.6	6.0	4.4	8.3
	2.00	2.78	N/A	N/A	4.7	6.3	5.0	9.0
Sub-Angular 50-70	0.0064	0.02	N/A	N/A	N/A	N/A	1.1	1.4
	0.25	0.96	N/A	N/A	2.5	4.4	2.5	4.7
	0.50	1.92	2.2	4.8	3.0	5.9	3.0	6.4
	1.00	3.85	N/A	N/A	3.8	8.0	3.8	12.8
	2.00	7.69	N/A	N/A	3.9	9.3	3.9	17.4

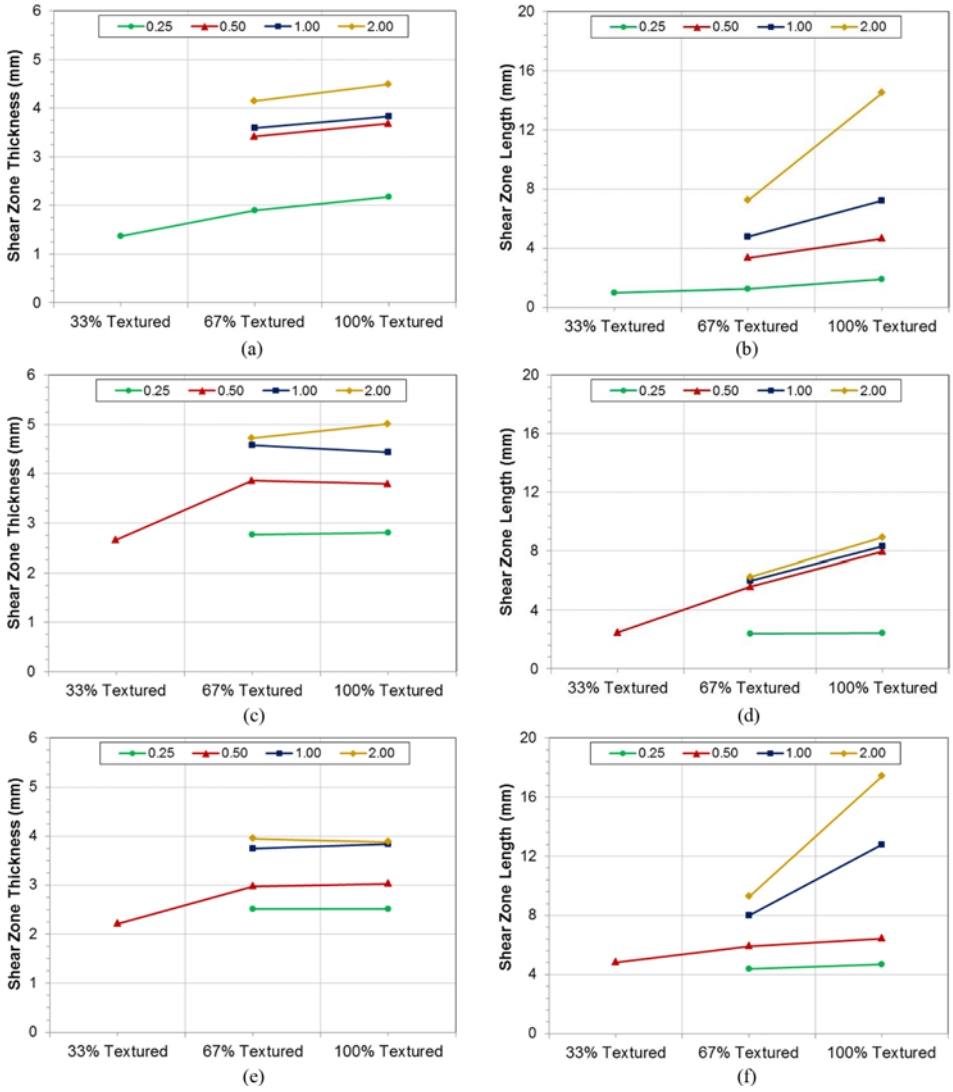

Fig. 12. Initiation and Progression of Shear Zone Thickness and Length as a Function of Percentage Textured Shearing for: (a) & (b) Sub-angular 20-30, (c) & (d) Sub-rounded 20-30 and (e) & (f) Sub-angular 50-70 Sands

shown in Figs. 12(b) and 12(f). The sub-rounded 20-30 sand (Fig. 12(d)) displays an approximately constant rate of shear zone deformation with increasing textured shear percentage for all tested surface roughnesses of R_{max} = 0.5 mm and greater. The noted differences in shear zone progression between the tested sands is attributed to the difference in particle angularity and the increase in particle rotation present in more rounded particle assemblies during interface shear. This conclusion is supported by the similarity in behavior of the two sub-angular sands of varying size, highlighting the greater dependence of shear zone length on particle angularity.

4. Discussion of Results

4.1 Granular Shearing Against Conventional Smooth Friction Sleeves

As noted by DeJong (2001) in an initial study of shear zone characteristics, interface shearing of sub-rounded 20-30 sand against conventional friction sleeves results in a pure sliding failure along the interface with no particle displacements noted even after 63.5 mm of relative displacement. The preserved post shear structure for such a test was shown in Fig. 6(b). The results of granular shearing against smooth CPT friction sleeves resulted in pure sliding for coarse sands, and only minor shear zone deformation in tests with a fine sand. Conventional CPT friction sleeves are standardized to a surface roughness value of R_a = 0.50 μm, whereas, in comparison, typical construction materials can have a very diverse range of surface roughness values (e.g. smooth geomembrane with $R_{max} \approx 1$ μm versus rough concrete with $R_{max} \approx 100$ μm). As the interface friction angle increases with increasing surface roughness, the shearing mechanism transitions from a pure sliding mechanism through an intermediate one of combined sliding and internal particle shearing to a maximum plateau in friction angle indicative of the full shear strength of the soil which is only mobilized when there is full internal particle shearing. Due to the transition of shearing mechanisms between sliding and internal shearing as a function of surface roughness, the interface strength can change up to 100% based on the surface roughness of typical construction and testing materials (Frost *et al.*, 2002). As such, it becomes imperative in geotechnical interface design to account not only for the construction material surface characteristics, but also to consider how they are affected by the surface characteristics of the testing device(s) used for subsurface characterization studies. This has been recognized by researchers (e.g., Lunne *et al.*, 1997) who pointed out the importance of monitoring the surface roughness of the conventionally used CPT friction sleeves. With use, the smooth friction sleeves tend to undergo wear and result in unintended effects in soil response measurement that is not routinely accounted for. This has been recognized by the authors as an additional source of variability in the f_s measurements which has in turn contributed to the tendency to use q_c measurements more often to determine soil properties.

4.2 Effect of Sleeve Roughness on Tests Against Textured Friction Sleeves

Surface roughness has been shown to be one of the most important factors affecting the strength of soil-geomaterial interfaces. The results of the current study confirm the transition in shearing mechanisms away from the interface and into the soil mass as surface roughness increases. The results presented in Figs. 9(a) and 9(b) and Figs. 10(a) through 10(d) showed that both the interface strength as well as the shear zone thickness increases with increased surface roughness for all three soils tested. The interface strength and shear zone thickness increases rapidly from that observed for smooth surfaces with the addition of moderate additional surface texture, and only moderate increases in shear zone thickness observed at values of $R_n \geq 1$ where the asperity height is greater than or equal to the mean particle diameter. An R_{max} between 0.50 and 1.00 mm, and an R_{max} of 0.25 mm, represents an $R_n \geq 1$ for the 20-30 and 50-70 sized sands, respectively. The addition of surface texture to the surface of friction sleeves proved to greatly affect the shear zone length, with shearing percentages of 23.0, 14.3, and 26.9% observed at the maximum surface roughness value of R_{max} = 2 mm for sub-angular 20-30, sub-rounded 20-30 and sub-angular 50-70 sands, respectively.

Uesugi and Kishida (1986a) reported a sharp transition from pure sliding to almost pure shearing for sand – steel interfaces under simple shear loading as a function of increased counterface roughness. They noted that for continuously textured interfaces, surfaces rough enough to induce shearing in the contacting granular soil resulted in predominantly shear failures with very little sliding. As noted earlier, pure shearing failures are undesirable for friction sleeves as this would clog the interface and result in changes in surface properties as a function of depth during penetration. This was taken into account in the design of the textured friction sleeves as noted earlier and the offset diamond texture was designed to be non-clogging. As noted by Uesugi *et al.* (1988), combined sliding and shearing is typical for heterogeneous surfaces comprised of both slide and shear inducing texture (i.e. both smooth and rough zones).

4.3 Effect of Particle Angularity on Tests Against Textured Friction Sleeves

Previous interface shear studies have shown that while particle angularity can have a large effect on interface strength (e.g., Potyondy, 1961; Brumund and Leonards, 1981), it has been shown to have a lesser effect on shear zone thickness (Frost *et al.*, 1999). While increases in particle angularity do not increase the thickness of induced shear zones, the void ratio inside shear bands of assemblies composed of angular particles is often higher, even exceeding global e_{max} locally at the contact surface. The current results confirm previous sentiment that angularity does not largely affect shear zone thickness, as sub-angular and sub-rounded 20-30 sands show equivalent thicknesses over all tested surface roughnesses. Only minor variations in shear zone thickness were noted between these sands, on the order of one

particle diameter, with the sub-rounded 20-30 sand exhibiting slightly thicker shear zones on average. However, this observation should be further addressed using soils of extreme angularities, such as highly rounded grains (e.g., glass beads) and highly angular grains (e.g., volcanic sands).

Particle angularity on the other hand had a defining effect on the shear zone length. Figs. 10(e) and 10(f) highlighted the divergence in the trends for the sub-angular and sub-rounded sands. This divergence was marked by an almost linearly increasing shear zone length with increasing surface roughness for the more angular sands, whereas the tests with the sub-rounded sand showed an upper bound for shear zone deformation at roughness levels of approximately $R_{max} \geq 0.5$ mm. It has long been noted in numerical (Boulon, 1989; Bardet, 1994; Mohamed and Gutierrez, 2010) and experimental (Oda *et al*., 1982; Kishida and Uesugi, 1987) studies that particle rotation becomes a large component of shear failure for rounded particles. While the experimental procedures used in this study provide no basis for tracking particle movements during shear, and thus no way to derive particle rotations, it is hypothesized that the divergence in shear zone length for rounded and angular particles is predominantly due to the greater resistance to rotation (i.e., rotational frustration) provided by angular particles, resulting in a larger particle displacement due to the lowest energy failure mechanism being slippage at particle-particle contacts.

4.4 Effect of Particle Size (D_{50}) on Tests Against Textured Friction Sleeves

Figures 10(a) through 10(d) showed the induced shear zone thickness as a function of surface roughness. These results contradict the classical notion that an induced shear zone within a granular assembly can be represented by a unique (or narrow range) multiple of particle diameter. The results clearly show that the fully developed shear zone for all three sands comprise a zone of almost equivalent thickness, of between 4 and 5 mm (Fig. 10(a)), but when expressed in terms of mean particle diameter the thickness magnitudes are significantly different, on the order of 6 to 7 D_{50} equivalents for the medium sands and 12 to 14 D_{50} equivalents for the fine sand (Fig. 10(b)). The maximum height roughness, R_{max}, showed to be a better roughness parameter in yielding a unifying trend within the data, as observed in Fig. 10(a). Although normalized roughness creates a unifying trend for interface strength, as shown by Uesugi and Kishida, 1986a, it did not for the shear zone thickness (Fig. 10(c)).

Figures 10(e) and 10(f) showed shear zone length as a function of surface roughness. The representative shear zone length for the sub-angular sands exhibited a relatively constant differential across the range of sleeve textures tested. As such the mean particle diameter seems to have only a minor influence on the shear zone length after the onset of shearing for sub-angular particles.

4.5 Comparison with In-Soil Shear Band Thickness

Researchers have hypothesized that interface shear zones are essentially equivalent to half of in-soil shear bands for relatively uniform sands (Frost *et al*., 2004). The thickness of interface shear zones is dependent on the properties of the continuum surface, whereas, in-soil shear zones are formed along a virtual surface comprised of soil particles. A compilation of shear band (half-width) and interface shear zone thicknesses in terms of D_{50} equivalents is shown in Fig. 13. Assuming the shear zone thickness at a roughness, R_{max}, equal to $\frac{1}{2} \cdot D_{50}$ for each of the three tested soils from the trends in Fig. 10(b), values of 4.3, 4.6, and 6.7 D_{50} are obtained for the sub-angular 20-30, sub-rounded 20-30 and sub-angular 50-70 sands, respectively. Fig. 13 shows these values superimposed on the previous shear zone thickness compilation. The superposition shows that the current results agree with the hypothesis that interface shear zones approximate half in-soil shear zones, and that continuum surface roughnesses on the order of $\frac{1}{2} \cdot D_{50}$ correlate well with the behavior of in-soil shear planes. These results show that for sands with a mean particle size smaller than about 0.6 mm, the shear zone thickness does not have a unique value in terms of D_{50} equivalents. On the other hand, the data shows for sands with a larger D_{50} the zone thicknesses can be described as about 4.3 D_{50} equivalents. This observation is in disagreement with results published by Ho, et al (2011), who presented shear zone thicknesses values that are independent of D_{50} for sands with mean particle sizes larger than about 0.9 mm. It should be pointed that the authors only reported shear zone thickness values of sands with D_{50} smaller than 1.5 mm, as opposed to the current study that includes sands of D_{50} as large as 2.5 mm. Additionally, the results presented in Fig. 13 show the independence of shear zone thickness from particle angularity, as thicknesses from both rounded and angular sands follow the same relationship. Additional studies are required to determine the precise reasons for these observations. However, it is believed that energy dissipation within the granular media in the form of frictional losses and geometrical attenuation plays an

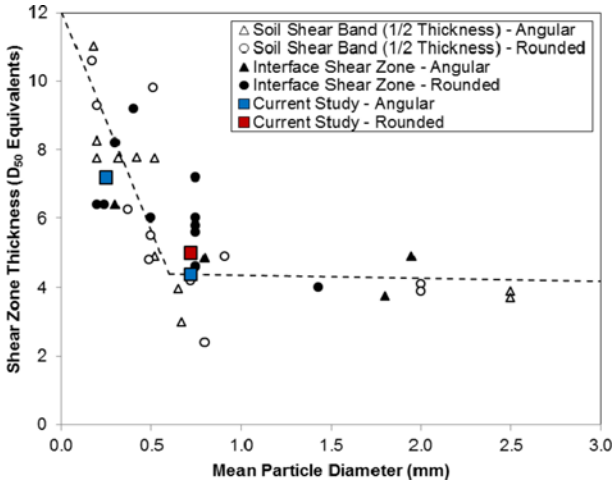

Fig. 13. Summary of Reported Shear Band (Half-Width) and Interface Shear Zone Thickness in Terms of: (a) D_{50} Equivalents, (b) Physical Distance (mm) (adapted after Frost *et al*., 2004)

important role on the volume of soil that is involved in the shear localization and shear banding processes.

4.6 Implications on Field Testing with Textured CPT Sleeves

The results of mobilized interface strength and shear zone thickness and length presented in Figs. 8(a) through 8(c), 9(a) through 9(d) and 10(a) through 10(f) indicate they are all significantly affected by the magnitude of the interface surface roughness. The tests with conventional smooth CPT sleeves resulted in minimal shear zone deformations and much lower mobilized interface strengths as compared to tests with textured sleeves. These results indicate that sliding between the sand grains and the smooth surface of the conventional smooth CPT sleeves is the principal failure mechanism and captured soil response.

As the sleeve's surface roughness increases, the induced shear deformations and mobilized shear strengths both increase. The friction sleeve-soil load transfer mechanisms are responsible for this relationship. As such, as the sleeve's surface roughness increases, larger asperities (i.e., higher diamond elements) engage a larger volume of soil, resulting in an increase in shear zone thickness and mobilized interface strength. Additionally, the shear zone length also increases as the failure mechanism changes from particle-surface sliding to soil shearing that is accompanied by significant shear-induced particle displacements and particle rotations. This enhanced soil engagement and shearing that makes the use of textured sleeves advantageous for in-situ testing. By introducing a non-clogging surface roughness texture it is possible to induce significant soil shearing that mobilizes loads that are recorded and provide a direct measurement of the soil shear strength, as opposed to the sliding failure mechanism captured by the conventional CPT f_s measurement or the empirical methods required to estimate soil strength from q_t measurements.

The volume of soil that is "sensed" by a given sensor also has important implications on the characteristics of its measurement, such as its resolution. Previous researchers have pointed out that the q_c measurement of the CPT senses a volume of soil that is in average 16 times the diameter of the probe (Lunne *et al*., 1997; Schmertmann, 1977). This results in an approximate sensed sphere of soil that has a diameter between 60 and 70 cm and a volume between 0.1 to 0.2 m^3, depending on the diameter of the CPT probe. Ahmadi and Robertson (2005) performed a detailed numerical study where they show the effects of this measurement averaging that takes place in a zone that is 10-20 times the diameter of the cone. By means of parametric numerical simulations, they concluded that the full tip resistance may not be reached in thin layers and provided correction factors for this. On the other hand, shearing against textured sleeves induces shear zones of thickness between 4 and 5 mm, as shown in Fig. 10(a). From simple geometry, the volume of this hollow cylinder of sheared soil is about 0.000075 m^3. This volume is three to four orders of magnitude smaller than that sensed by the q_c measurement, and thus enables for a measurement of soil response which has a much higher resolution and provides more detailed information, especially in highly stratified ground profiles, as shown by Saussus *et al.* (2004) through numerical simulations.

5. Conclusions

The current study included a series of tests to investigate the micromechanical response of a variety of granular materials sheared against both smooth and rough surfaced friction sleeves that are used with multi-sleeve friction attachments for CPT-based exploration. The following conclusions can be drawn from the experimental results:

1. Interface shearing of coarse granular media against conventional smooth friction sleeves did not induce a shear zone, and resulted in a pure sliding mechanism under the current test conditions. These results agree with previous studies such as DeJong (2001). Interface shearing of fine sands against, interface shearing of fine sand against conventional smooth friction sleeves was shown to induce a minimal shear zone, and resulted in a combined failure mechanism consisting of mostly (98%) sliding deformation under the current test conditions.
2. The offset diamond texturing pattern used to add varying levels of surface roughness to friction sleeves has been experimentally verified to induce non-clogging shear across the range of sleeve roughnesses and granular soils tested. Also, the texture pattern proved to produce shear zones of approximately uniform thickness for all soils tested, uniform length for the medium-sized sands and relatively non-uniform length for the fine sand.
3. Interface surface roughness, R_{max}, has been shown to have a dominant effect on induced interface shear zone thickness as compared to the sand size and angularity. This is in contrast to the behavior of internal shear zones, and results from the uniqueness of internal "virtual roughness" as compared to the non-uniqueness of interface roughness with respect to the contacting particulate properties.
4. The current results and findings corroborate previous accounts of the independence of interface shear zone thickness and granular particle angularity; however, the extent of shear zone length was shown to be largely dependent on particle angularity for roughness values above a critical value. Rounded particles exhibited an upper limit of shear displacement with increased interface roughness, while more angular particles exhibited an approximately linear trend between shear deformation and interface roughness over the range of roughnesses tested.
5. It is believed that sleeves using the offset texturing scheme can be used to successfully investigate the complete range of typically encountered interface strengths. This study has served to not only further validate the effectiveness of the current textured sleeves for investigating interface behavior in-situ, but has also further advanced the fundamental understanding of the micromechanical interface interactions necessary to fully understand the behavior of smooth and

textured continuum surfaces placed in contact with placed in contact with soils.

6. The current texturing scheme has been experimentally shown to induce interface shear zones equivalent to those reported induced by continuous texture. The critical roughness required to induce full shear zones for the current intermittent texturing scheme ($R_n \approx 1$) is increased by an order of magnitude over that typically required for continuous texturing ($R_n \approx 0.1$). The amount of R_n roughness necessary to fully engage the internal resistance of the contacting particulate ("$\delta = \phi$" condition) is believed to be dependent on the spacing and other characteristics of the texture.
7. The results show that increasing friction sleeve surface roughness results in an increase of mobilized peak and residual interface strengths. As the friction sleeve's surface roughness is increased (i.e., as the diamond asperities become higher), a larger volume of soil is engaged during shearing. Thus, larger shear zone thicknesses and interface strengths are mobilized. Additionally, the failure mechanisms changes from particle-sleeve sliding to soil shearing that result in larger shear zones as the surface roughness is increased. These results present important implications for field testing conditions. For instance, shearing against textured sleeves provides a direct measurement of the soil strength, as opposed to the sliding mechanisms captured by f_s readings or the need for empirical methods used to estimate soil properties from q_c readings. Also, the volume of soil "sensed" in shearing against textured sleeves is four orders of magnitude smaller than that "averaged" in the q_c measurement. This makes the former a measurement with a much higher resolution for stratigraphic profiling. It should be noted that these results are based on controlled laboratory-scale studies although field tests with textured sleeves support these observations. While important insights were obtained regarding the soil-friction sleeve interactions, these must be used with care in order to apply them to field conditions. Also, the effect of testing parameters such as sand relative density, magnitude of confining stress and magnitude of sleeve displacement were not directly investigated. A research program that addresses these factors is currently ongoing.

Acknowledgements

This research was partially supported by National Science Foundation grant #CMS-9978630, and the first author was supported by a National Defense Science and Engineering Graduate Fellowship while at Georgia Tech. Both sources of support are gratefully acknowledged.

References

Ahmadi, M.M. and Robertson, P.K. (2005). "Thin-layer effect on the CPT q_c measurement." *Canadian Geotechnical Journal*, 42, No. 5, pp. 1302-1317, DOI: 10.1139/T05-036.

ASTM D 5321-14 (2014). *Standard test method for determining the shear strength of soil-geosynthetic and geosynthetic-geosynthetic interfaced by direct shear*, West Conshohocken, PA.

ASTM D 5778-12 (2012). *Standard test method for performing electronic friction cone and piezocone penetration testing of soils*, West Conshohocken, PA.

Bardet, J. P. (1994). "Observations on the effect of particle rotations on the failure of idealized granular materials." *Journal of Mechanics of Materials*, Vol. 18, No. 2, pp 159-182, DOI: 10.1016/0167-6636 (94)00006-9.

Boulon, M. (1989). "Basic features of soil-structure interface behavior." *Computers and Geotechnics*, Vol. 7, Nos. 1-2, pp. 115-131.

Brumund, W. F. and Leonards, G. A. (1973). "Experimental study of static and dynamic friction between sand and typical construction materials." *ASTM Journal of Testing and Evaluation*, Vol. 1, No. 2, pp. 162-165, DOI: 10.1520/JTE10893J.

Cargill, P. E. (1999). *The influence of friction sleeve roughness on cone penetration measurements*, MSc Thesis, Georgia Institute of Technology, Atlanta.

DeJong, J. T. (2001). *Investigation of particulate-continuum interface mechanics and their assessment through a multi-friction sleeve penetrometer attachment*, PhD Dissertation, Georgia Institute of Technology, Atlanta, May.

DeJong, J. T. and Frost, J. D. (2002). "A multi-friction sleeve attachment for the cone penetrometer." *ASTM Geotechnical Testing Journal*, Vol. 25, No. 2, pp. 111-127, DOI: 10.1520/GTJ11355J.

DeJong, J. T., Frost, J. D., and Cargill, P. E. (2001). "Effect of surface texturing on CPT friction sleeve measurements." *Journal of Geotechnical and Geoenvironmental Engineering*, Vol. 127, No. 2, pp. 158-168, DOI: 10.1061/(ASCE)1090-0241(2001)127:2(158).

DeJong, J. T., Frost, J. D., and Sacs, M. (2000). "Relating quantitative measures of surface roughness and hardness to geomaterial interface strength." *Proc., Geo-Eng 2000*, Sydney, AUS.

DeJong, J. T., Frost, J. D., and Saussus, D. R. (2002). "Relative aspect of surface roughness at particulate-solid interfaces." *ASTM Journal of Testing and Evaluation*, Vol. 30, No. 1, pp. 8-19, DOI: 10.1520/GTJ11355J.

Dietz, M. S. and Lings, M. L. (2006). "Postpeak strength of interfaces in a stress-dilatancy framework." *Journal of Geotechnical and Geoenvironmental Engineering*, Vol. 132, No. 11, pp. 1474-1484, DOI: 10.1061/(ASCE)1090-0241(2006)132:11(1474).

Dove, J. E. and Frost, J. D. (1999) "Peak friction behavior of smooth geomembrane-particle interfaces." *Journal of Geotechnical and Geoenvironmental Engineering*, Vol. 125, No. 7, pp. 544-555, DOI: 10.1061/(ASCE)1090-0241(1999)125:7(544).

Dove, J. E., Frost, J. D., Han J., and Bachus, R. C. (1997). "The influence of geomembrane surface roughness on interface strength." *Proc., Geosynthetics '97*, Vol. 2, pp. 863-876.

Frost, J. D. and Han, J. (1999). "Behavior of interfaces between fiber-reinforced polymers and sands." *Journal of Geotechnical and Geoenvironmental Engineering*, Vol. 125, No. 8, pp. 633-640, DOI: 10.1061/(ASCE)1090-0241(1999)125:8(633).

Frost, J. D. and Lee, S. W. (2001). "Microscale study of geomembrane-geotextile interactions." *Geosynthetics International*, Vol. 8, No. 6, pp. 577-597, DOI: 10.1680/gein.8.0207.

Frost, J. D. and Martinez, A. (2013). "Multi-sleeve axial-torsional-piezo friction penetration system for subsurface characterization." *Proc., of the 18th ISSMGE International Conference on Soil Mechanics*

and Geotechnical Engineering, Paris, France. pp. 527-530.

Frost, J. D., and DeJong, J. T. (2001). "A new multi-friction sleeve attachment." *Proc., 15th International Conference on Soil Mechanics and Geotechnical Engineering*, Istanbul, 1, pp. 91-94.

Frost, J. D., and DeJong, J. T. (2005). "In situ assessment of the role of surface roughness on interface response." *Journal of Geotechnical and Geoenvironmental Engineering*, Vol. 131, No. 4, pp. 498-511, DOI: 10.1061/(ASCE)1090-0241(2005)131:4(498).

Frost, J. D., DeJong, J. T. and Recalde, M. (2002). "Shear failure behavior of granular-continuum cnterfaces." *Engineering Fracture Mechanics*, Vol. 69, No. 17, pp. 2029-2048, DOI: 10.1016/S0013-7944(02) 00075-9.

Frost, J. D., Hebeler, G. L, Evans, T. M., and DeJong, J. T. (2004). "Interface behavior of granular soils." *Proc., Earth and Space, 9th Biennial ASCE Aerospace Division International Conference on Engineering, Construction, and Operations in Challenging Environments*, Houston, TX, pp. 65-72.

Frost, J. D., Lee, S., and Cargill, P. E. (1999). "The evolution of sand structure adjacent to geomembranes." *Proc., Geosynthetics '99*, Vol. 1, pp. 559-573.

Ghionna, V. and Jamiolkowski, M. (1991). "A critical appraisal of calibration chamber testing of sands." *Proc., 1st International Symosium. On Calibration Chamber Testing (ISOCCT1).* Elsevier, Potsdam, N.Y., pp. 13-39.

Gokhale, A.M. and Drury, W.J. (1990). "A general method for estimation of fracture surface roughness: Part II. Practical Considerations." *Metallurgical Transactions*, A, Vol. 21A, No. 5, pp. 1201-1207, DOI: 10.1007/BF02656539.

Hebeler, G. L. (2005). "Multi scale investigations of interface behavior." PhD Dissertation. *Georgia Institute of Technology*, Atlanta, 772 pp.

Hebeler, G. L. and Frost, J. D. (2006). "A multi piezo-friction attachment for penetration testing." *Proc., ASCE Geo-Institute Congress: Geotechnical Engineering in the Information Technology Age*, Atlanta, pp. 1-6.

Ho, T. Y. K, Jardine, R. J., and Anh-Minh, N. (2011). "Large-displacement interface shear between steel and granular media." *Géotechnique*, 61, No. 3, pp. 221-234, DOI: 10.1680/geot.8.P.086.

Hryciw, R. D. and Irsyam, M. (1993). "Behavior of sand particles around rigid ribbed inclusions during shear." *Soils and Foundations*, Vol. 33, No. 3, pp. 1-13.

ISSMFE (1989). "International reference test procedure for cone penetration test (CPT)." Report of the ISSMFE technical committee on penetration testing of soils - TC 16, with reference to test procedures, *Swedish Geotechnical Institute*, Linkoping, Information, No. 7, pp. 6-16.

Jardine, R. J. and Chow, F. C. (1996). "New design methods for offshore piles." *MDT Publications 96/103, Marine Technology Directorate*, London.

Jardine, R. J. and Lehane, B. M. (1993). *Research into the behavior of offshore piles: Field experiments in sand and clay*, Offshore Technology Report 93-401, HSE Books.

Kishida, H. and Uesugi, M. (1987). "Test of the interface between sand and steel in the simple shear apparatus," *Géotechnique*, Vol. 37, No. 1, pp. 45-52, DOI: 10.1680/geot.1987.37.1.45.

Lee, S. W. (1998). "Influence of Surface topography on interface strength and counterface soil structure." PhD Dissertation, *Georgia Institute of Technology*, Atlanta.

Lehane, B. M. and Jardine, R. J. (1994). "Displacement pile behaviour in a glacial clay." *Canadian Geotechnical Journal*, Vol. 31, No. 1, pp. 79-90, DOI: 10.1139/t94-009.

Lunne, T., Robertson, P. K., and Powell, J. J. M. (1997). *Cone Penetrating Testing In Geotechnical Practice*, New York: Blackie Academic, EF Spon/Routledge Publishers.

Martinez, A., Frost, J. D., and Su, J. (2015). "The importance of interfaces in geotechnical foundation systems." *Proc. International Foundations Congress and Equipment Expo., IFCEE*. San Antonio, pp. 817-526. DOI: 10.1061/9780784479087.074.

Mitchell, J. K. and Villet, W. C. B. (1987). "Reinforcement of earth slopes and embankments" *National Cooperative Highway Research Program Report 290*, Washington, D.C.: Transportation Research Board of the National Research Council.

Mohamed, A. and Gutierrez, M. (2010). "Comprehensive study of the effect of rolling resistance on the stress-strain localization behavior of granular materials." *Granular Matter*, Vol. 12, No. 5, pp. 527-541, DOI: 10.1007/s10035-010-0211-x.

Oda, M., Konishi, J., and Nemat-Nasser, S. (1982). "Experimental micromechanical evaluation of strength of granular materials: Effects of particle rolling." *Mechanics of Materials*, Vol. 1, No. 4 pp. 269-283, DOI: 10.1016/0167-6636(82)90027-8.

Potyondy, J. G. (1961). "Skin friction between various soils and construction materials." *Géotechnique*, Vol. 11, No. 4, pp. 339-353, DOI: 10.1680/geot.1961.11.4.339.

Saussus, D. R., Frost, J. D., and DeJong, J. T. (2004). "Statistical analysis of friction sleeve length effects on soil classification." *International Journal for Numerical and Analytical Methods in Geomechanics*, Vol. 28, No. 12, pp. 1257-1278, DOI: 10.1002/nag.386.

Schmertmann, J. (1977). "Guidelines for cone penetration test: performance and design." *Dept. of Transportation Federal Highway Administration, Offices of Research and Development*, Washington.

Uesugi, M. and Kishida, H. (1986a). "Influential factors of friction between steel and dry sands." *Soils and Foundations*, Vol. 26, No. 2, pp. 33-46.

Uesugi, M. and Kishida, H. (1986b). "Frictional resistance at yield between dry sand and mild steel." *Soils and Foundations*, Vol. 26, No. 4, pp. 139-149.

Uesugi, M., Kishida, H., and Tsubakihara, Y. (1988). "Behavior of sand particles in sand-steel friction." *Soils and Foundations*, Vol. 28, No. 1, pp. 107-118.

Wang, J., Gutierrez, M. S., and Dove, J. E. (2007). "Numerical studies of shear banding in interface shear tests using a new strain calculation method." *International Journal for Numerical and Analytical Methods in Geomechanics*, Vol. 31, No. 12, pp. 1349-1366, DOI: 10.1002/nag.589.

Ward, H. C. (1999). *Rough surfaces*, Thomas, T.R., Ed., Longman, London, 278 pp.

White, D. J., Take, W. A., Bolton, M. D., and Munachen, S. E. (2001). "A deformation measuring system for geotechnical testing based on digital imaging, close range photogrammetry and PIV image analysis." *Proc., 15th International Conference on Soil Mechanics and Geotechnical Engineering*, Istanbul, pp. 539-542.

Yoshimi, Y. and Kishida, T. (1981a). "A ring torsion apparatus for evaluating friction between soil and metal surfaces." *ASTM Geotechnical Testing Journal*, Vol. 4, No. 4, pp. 145-152, DOI: 10.1520/GTJ10783J.

Yoshimi, Y. and Kishida, T. (1981b). "Friction between sand and metal surfaces." *Proc., 10th International Conference on Soil Mechanics and Foundation Engineering*, Stockholm, Vol. 1, pp. 831-834.